Journal of Chemical Crystallography
https://doi.org/10.1007/s10870-020-00834-5

ORIGINAL PAPER

Synthesis and Crystal Structure of a 6H Hexagonal Fluoro-Perovskite: $RbMgF_3$

Mohammad Usman[1] · Gyanendra B. Ayer[1] · Mark D. Smith[1] · Hans-Conrad zur Loye[1]

Received: 10 November 2019 / Accepted: 5 May 2020

Abstract

$RbMgF_3$, a perovskite halide, serendipitously crystallized from a reaction between $MgCl_2$ and TiO_2 in molten RbCl/RbF eutectic flux (melting point = 546 °C) and was characterized by single crystal X-ray diffraction. $RbMgF_3$ crystals can also be grown directly in higher yield using a molten RbCl–RbF flux layered over $MgCl_2$ or MgF_2 contained in a silver tube at 575 °C. $RbMgF_3$ crystallizes in the hexagonal space group $P6_3/mmc$ in the 6H hexagonal perovskite structure type with lattice parameters $a = 5.8368(2)$ Å and $c = 14.2087(5)$ Å. The crystal structure exhibits face-sharing Mg_2F_9 octahedra connected via corner-sharing MgF_6 octahedra. Elemental composition for $RbMgF_3$ was semi-quantitatively confirmed by energy dispersive spectroscopy (EDS).

Graphic Abstract

X-ray diffraction quality single crystals of RbMgF3 were grown from a molten RbCl/RbFeutectic flux at 850 °C and used for structure determination using single crystal X-raydiffraction. The compound crystallizes in the hexagonal space group *P63/mmc* in the 6Hhexagonal structure type.

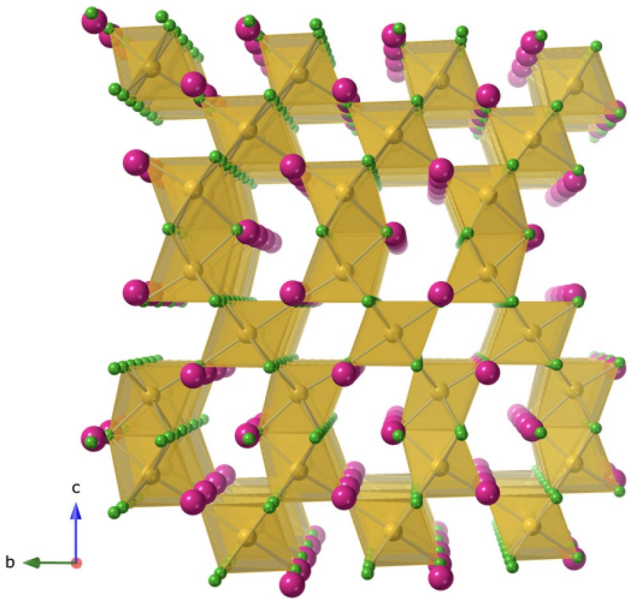

Keywords $RbMgF_3$ · Crystal growth · Perovskite halide materials

✉ Hans-Conrad zur Loye
zurloye@mailbox.sc.edu

[1] Department of Chemistry and Biochemistry, University of South Carolina, Columbia, SC 29208, USA

Published online: 12 May 2020

Introduction

Halide perovskites have attracted significant attention over the past several years due to their attractive optical properties that make them excellent candidates for solar energy conversion. Most halide perovskites investigated contain an organic cation, although more recently "pure" halide perovskites have been synthesized and reported. Most of that work has focused on double perovskite structures, however, the synthesis and characterization of perovskite halides of the type ABX_3 remain of interest [1–4].

ABX_3 perovskite halides are being investigated for applications other than solar energy, however. Specifically, their optical behavior can be tailored for specific applications via doping on the A or B sites. For example, the title compound, $RbMgF_3$, can be doped with transition metal ions to make it useful for applications in optically-induced luminescence and radiation detectors [5, 6]. Moreover, temperature-tunable upconversion luminescence was observed in the series of $KZn_{0.99-x}F_3{:}0.01Yb^{3+},xMn^{2+}$ ($x = 0$, 0.01, 0.025,0.075, 0.10, 0.15 and 0.20 mol) samples synthesized by a rational hydrothermal method [7]. Cases also exist where the *B*-site in $RbMgF_3$ was doped with a small rare-earth, such as Yb^{3+}, and the consequent study of the paramagnetic centers formed by the Yb^{3+} ions was carried out via EPR and optical spectroscopy [8].

Polycrystalline samples of $RbMgF_3$ and doped $RbMgF_3$ have been prepared and investigated for their optical properties, including scintillation. Interestingly, no high quality single crystal structure of this well-known fluoro-perovskite has been reported; however, based on Weissenberg precession images that established the unit cell, and by assuming that $RbMgF_3$ and $RbNiF_3$ are isostructural, the general structure of the compound has been reported [9]. Recently, Szlag et al. reported a facile route to preparing the hexagonal and cubic polymorphs of polycrystalline $RbMgF_3$, structurally characterized via Rietveld refinement [10]. Briefly, the solid-state and solution thermolysis of $Rb_2Mg_2(tfa)_6(tfaH)_2{\cdot}3H_2O$ carried out by Szlag et al. provided access to the hexagonal and cubic polymorphs of $RbMgF_3$, respectively.

A number of 6H perovskites are known, the most famous being doped $BaTiO_3$; however, the list includes many other oxides and halides [11–16]. The reason for the formation of the 6H vs the regular cubic ABX_3 perovskite has to do with the size of the A, B and X ions, as defined by the Goldschmidt tolerance factor [17]. An A cation that is, relatively speaking, too large for B and X, pushes the structure toward the 2H-hexagonal perovskite variant [18–21]. Hence, while $KMgF_3$ crystallizes in the cubic structure, [22] the title compound, $RbMgF_3$, with a noticeably larger A cation, crystallizes in the 6H perovskite variant.

Herein, we report on the crystal structure of the hexagonal polymorph of $RbMgF_3$ which formed as a minor side product in a reaction targeted to crystallize a Rb/Mg/Ti/O hollandite [23]. Alternatively, significant yield of single crystals can be obtained directly from a molten RbCl–RbF flux at 575 °C. The crystal growth conditions and structure determination for $RbMgF_3$ are detailed in this paper.

Experimental

Synthesis

$MgCl_2$ (Fisher Scientific), TiO_2 (Rutile, 99.9%, Alfa Aesar), RbCl (99%, Alfa Aesar), and RbF (99.1%, Alfa Aesar) were used for the flux growth synthesis of $RbMgF_3$.

Single crystals of $RbMgF_3$ formed using a molten RbCl–RbF eutectic flux (melting point = 546 °C) layered over $MgCl_2$ and TiO_2. Precisely, 1 mmol of $MgCl_2$ and 1 mmol of TiO_2 was placed beneath a mixture of 1.2 g of RbCl-RbF mix in a 7.5 cm tall by 1.2 cm diameter cylindrical silver crucible with one of its ends sealed and welded shut using a TIG-175 Square Wave Lincoln Electric welder. The other end of the crucible containing the charge was crimped shut and the loaded crucible was placed into a programmable furnace. The reaction mixture was heated at 600 °C/h to 850 °C, maintained at this temperature for 12 h, slow cooled to 500 °C at 10 °C/h, and then rapidly cooled to room temperature by shutting the furnace off. Once cooled to ambient temperature, the solidified RbCl–RbF flux was dissolved in water, aided by sonication, and the resulting products were isolated via vacuum filtration. Irregular colorless plate crystals of $RbMgF_3$ formed as a minor phase together with the Rb–Ti–Mg–O hollandite, the major phases.

It is also possible to prepare $RbMgF_3$ crystals using a molten RbCl–RbF flux layered over $MgCl_2$ or MgF_2 contained in a silver tube. A reaction mixture consisting of 2 mmol of MgF_2, 3 mmol of RbF, and 2 mmol of RbCl was heated at 575 °C for 24 h and cooled to 300 °C at a rate of 10 °C/h. The reaction resulted in a mixture of $RbMgF_3$ and Rb_2MgF_4.

Characterization

Single Crystal X-ray Diffraction

X-ray intensity data from an irregular colorless plate were collected at 301(2) K using a Bruker D8 QUEST diffractometer equipped with a PHOTON 100 CMOS area detector and an Incoatec microfocus source (Mo $K\alpha$ radiation, $\lambda = 0.71073$ Å) [24]. The data collection covered 100% of reciprocal space to $2\theta_{max} = 75.6°$, with an average reflection

redundancy of 37.9 and $R_{int} = 0.051$ after absorption correction. The raw area detector data frames were reduced, scaled and corrected for absorption effects using the SAINT + and SADABS programs [24, 25]. Final unit cell parameters were determined by least-squares refinement of 9972 reflections taken from the data set. An initial structural model was obtained with SHELXT [26]. Subsequent difference Fourier calculations and full-matrix least-squares refinement against F^2 were performed with SHELXL-2018 [27] using the ShelXle interface [28].

The compound crystallizes in the hexagonal system. The space group $P6_3/mmc$ was consistent with the pattern of systematic absences in the intensity data and was confirmed by structure solution. The asymmetric unit consists of two rubidium atoms, two magnesium atoms and two fluorine atoms. All atoms are located on special positions. Rb(1) and Mg(1) occupy site 4*f* (3 *m*. site symmetry), Rb(2) occupies site 2*b* (− 6*m*2 symmetry), Mg(2) occupies site 2*a* (− 3 *m*. symmetry), F(1) is on site 12 *k* (.*m*. symmetry) and F(2) is on site 6 *h* (*mm*2 symmetry). All atoms were refined with anisotropic displacement parameters. All atoms refined to full occupancy. The largest residual electron density peak and hole in the final difference map are + 0.48 and − 0.85 $e^-/Å^3$, located 1.60 Å and 1.05 from Rb(1), respectively.

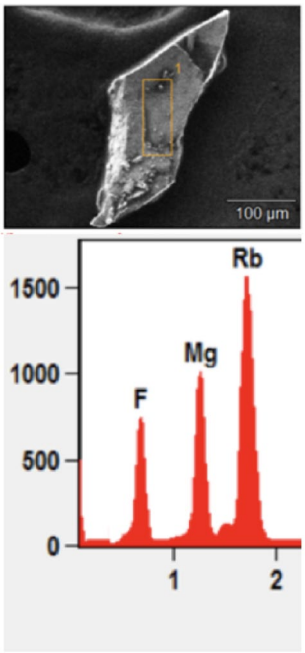

Fig. 1 SEM image (top) and EDS spectrum (bottom) for $RbMgF_3$. Rb, Mg and F, by atomic composition, were detected in 18.22%, 21.34% and 60.44%, respectively

Energy Dispersive Spectroscopy

EDS was performed on an irregular colorless plate using a TESCAN Vega-3 SBU scanning electron microscope (SEM) with a Thermo EDS attachment operated in an ultralow vacuum mode. The crystal was mounted on an SEM stub with carbon tape and analyzed using 20 kV accelerating voltage and an accumulation time of 20 s. EDS verified the presence of Rb, Mg and F in an approximately 1:1:3 ratio. Figure 1 illustrates the EDS spectrum for $RbMgF_3$.

Results and Discussion

Many inorganic fluorides have been prepared via mild hydrothermal routes, which utilize superheated water as the solvent for crystallization and hydrofluoric acid as a fluorinating and complexing agent [29]. Another approach for the crystal growth of fluorides is molten salt flux crystal growth, a well-established and viable synthetic route to prepare complex fluorides [30], although many phases that are obtained using this approach are oxy-fluorides [31–33].

Single crystals of $RbMgF_3$ were grown out of a molten RbCl–RbF eutectic flux together with crystals of a rubidium containing magnesium-titanate hollandite structure. $RbMgF_3$ crystallized as irregular colorless plates. Once the $RbMgF_3$ crystals had been identified and structurally characterized using single crystal X-ray diffraction, attempts were made to rationally synthesize this phase by combining MgF_2 or $MgCl_2$ as the magnesium precursor in a molten RbCl–RbF eutectic flux. This led to the formation of $RbMgF_3$ crystals, as well as mm-sized, nicely faceted, plate-like crystals of Rb_2MgF_4 [34]. Combining $MgCl_2$ and RbCl in molten NaCl–NaF eutectic melt mainly yielded silver chloride powder (from the silver ampoule) and few plate-like crystals that were identified as $NaMgF_3$.

$RbMgF_3$ crystallizes in the hexagonal space group $P6_3/mmc$, characteristic of 6H hexagonal perovskites. Crystallographic and refinement data for $RbMgF_3$ can be found in Table 1. Atomic coordinates are listed in Table 2 and selected interatomic distances are provided in Table 3. The compound exhibits two unique rubidium atoms, two unique magnesium atoms and two unique fluorine atoms. Both magnesium atoms are found in octahedral environments. Mg(1) is coordinated to three F(1) atoms and three F(2) with bond distances of 1.9826(8) Å and 2.0229(9) Å respectively. Mg(2) is coordinated to six F(1) atoms via six equal bonds having a bond length of 2.0253(7) Å. Both rubidium atoms exhibit a 12-fold coordination environment. Rb(1) is bonded to three F(2) atoms and nine F(1) with bond lengths of 2.8687(7) Å and 2.93040(12) – 3.0448(8) Å respectively; Rb(2) is bonded to six F(1) and six F(2) with bond lengths of 2.9440(8) Å and 2.92594(13) Å respectively. These bond distances are in decent agreement with the previously reported values [10]. Figure 2 illustrates the local coordination environment of the rubidium cations in $RbMgF_3$.

Table 1 Crystallographic and refinement data for $RbMgF_3$

Formula	$RbMgF_3$
Crystal color and habit	Colorless plates; irregular
Formula weight (g mol^{-1})	166.78
Temperature (K)	301(2)
Space group	$P6_3/mmc$
a (Å)	5.8368(2)
c (Å)	14.2087(5)
V (Å^3)	419.21(3)
Z	6
Density (g cm^{-3})	3.964
Crystal size (mm × mm × mm)	0.240 × 0.200 × 0.080
θ_{max} (deg)	37.798
Reflections collected	18,741
Goodness-of-fit on F^2	1.240
R indices [I > 2sigma(I)]	$R_1 = 0.0188$; $wR_2 = 0.0381$
Largest diff. peak and hole (e^- and Å^{-3})	0.483 and − 0.855

Table 2 Atomic coordinates (× 10^4) and equivalent isotropic displacement parameters (Å^2 × 10^3) for $RbMgF_3$

Atom	x	y	z	Ueq [Å^2]
Rb(1)	3333	6667	984(1)	15(1)
Rb(2)	0	0	2500	15(1)
Mg(1)	6667	3333	1526(1)	11(1)
Mg(2)	0	0	0	11(1)
F(1)	3320(1)	1660(1)	798(1)	16(1)
F(2)	5208(1)	415(2)	2500	14(1)

U(eq) is defined as one third of the trace of the orthogonalized U^{ij} tensor

Table 3 Interatomic distances (Å) of cation coordination spheres in $RbMgF_3$

Bond	Distance
Mg(1) – F(1) (×3)	1.9826(8)
Mg(1) – F(2) (×3)	2.0229(9)
Mg(1) – F(1) (×6)	2.0253(7)
Rb(1) – F(1) (×6)	2.93037(12)
Rb(1) – F(1) (×3)	3.0448(8)
Rb(1) – F(2) (×3)	2.8687(7)
Rb(2) – F(1) (×6)	2.9440(8)
Rb(2) – F(2) (×6)	2.92594(13)

$RbMgF_3$, typical of the 6H hexagonal structure type, features face-sharing Mg_2F_9 octahedra that are linked via corner-sharing MgF_6 octahedra to form a three-dimensional anionic framework charge balanced by the rubidium ions residing in the framework tunnels. A projection of the crystal structure of $RbMgF_3$ down the a-axis is shown in Fig. 3.

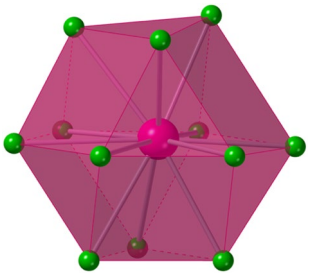

Fig. 2 12-fold coordination environment of the rubidium cation in $RbMgF_3$

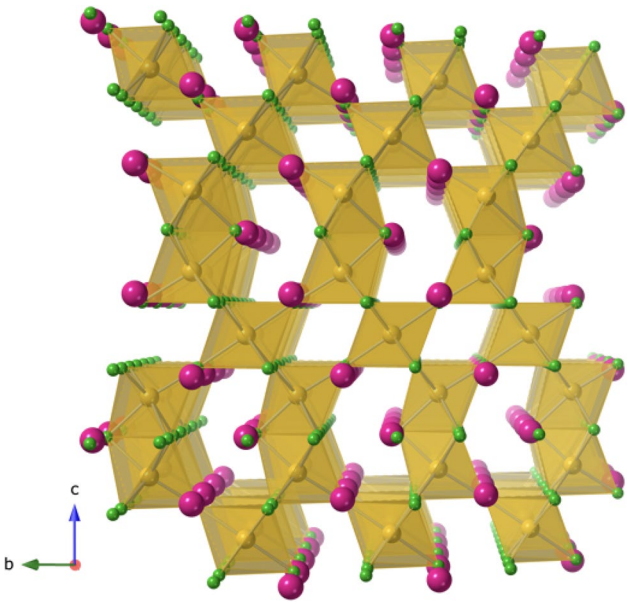

Fig. 3 Projection of the 6H hexagonal crystal structure of $RbMgF_3$ down the a-axis. Rb, Mg and F are shown in magenta, gold and lime, respectively

Conclusion

$RbMgF_3$, a 6H hexagonal fluoro-perovskite, crystallized out of a RbCl–RbF eutectic melt. The compound crystallizes in space group $P6_3/mmc$.

Supporting Information

Further details of the crystal structure investigation can be obtained from the Fachinformationszentrum Karlsruhe, 76344 Eggenstein-Leopoldshafen, Germany

(fax: + 497247808666; e-mail: crystdata@fiz-karlsruhe.de) on quoting the depository number 1948839.

Acknowledgements The authors gratefully acknowledge the U.S. National Science Foundation through grants DMR-1806279, OIA-1632881, and OIA-1655740.

References

1. Hao F, Stoumpos CC, Cao DH, Chang RPH, Kanatzidis MG (2014) Nat Photonics 8:488–494
2. Slavney AH, Hu T, Lindenberg AM, Karunadasa HI (2016) J Am Chem Soc 138(7):2138–2141
3. Yi C, Luo J, Meloni S, Boziki A, Ashari-Astani N, Grätzel C, Zakeeruddin SM, Röthlisberger U, Grätzel M (2016) Energy Environ Sci 9:656–662
4. Wu Z, Ji C, Wang S, Zhang W, Wang Y, Li L, Zhao S, Sun Z, Luo J (2017) J Mater Chem C 5:11466–11471
5. Dotzler C, Williams GVM, Rieser U, Robinson J (2009) J Appl Phys 105:023107
6. Williams GVM, Raymond SG (2011) Radiat Meas 46:1102
7. Song EH, Ding S, Wu M, Ye S, Xiao F, Dong GP, Zhang QY (2013) J Mater Chem C 1:4209–4215
8. Falin ML, Latypov VA, Leushin AM, Safiullin GM (2018) J Alloys Compd 735:23–28
9. Kerkouri N, Dance JM (1984) Mater Res Bull 19:751–757
10. Szlag RG, Suescun L, Dhanapala BD, Rabuffetti FA (2019) Inorg Chem 58:3041–3049
11. Zhao JG, Yang LX, Yu Y, Li FY, Yu RC, Fang Z, Chen LC, Jin CQ (2007) J Solid State Chem 10:2816–2823
12. Keith GM, Rampling MJ, Sarma K, Mc Alford N, Sinclair DC (2004) J Eur Ceram Soc 6:1721–1724
13. Arevalo-Lopez AM, Reeves SJ, Attfield JP (2014) Z Anorg Allg Chem 640:2727–2729
14. Valant M, Arčon I, Mikulska I, Lisjak D (2013) Chem Mater 25(17):3544–3550
15. Zhao JG, Yang LX, Yu Y, Li FY, Yu RC, Jin CQ (2008) J Solid State Chem 8:1767–1775
16. Schmidt RE, Welsch M, Kummer-Dörner S, Babel DZ (1999) Anorg Allg Chem 625(4):637–642
17. Goldschmidt VM (1926) Naturwissenschaften 14:477–485
18. Giaquinta DM, zur Loye HC (1994) Chem Mater 6:365–372
19. Ferreira T, Carone D, Huon A, Herklotz A, Stoian SA, Heald SM, Morrison G, Smith MD, zur Loye HC (2018) Inorg Chem 57:7362–7371
20. zur Loye HC, Zhao Q, Bugaris DE, Chance WM (2012) CrystEngComm 14:23–39
21. Stitzer KE, Smith MD, Gemmill WR, zur Loye HC (2002) J Am Chem Soc 124:13877–13885
22. Demartin F, Campostrini I, Castellano C, Russo M (2014) Phys Chem Miner 41:403–407
23. Usman M, Kocevski V, Smith MD, Morrison G, Besmann T, zur Loye HC (2020) Cryst Growth Des 20(4):2398–2405
24. APEX3 Version 2016.5-0 and SAINT+ Version 8.37A (2016) Bruker AXS, Inc., Madison, Wisconsin, USA
25. SADABS-2016/2: Krause L, Herbst Irmer R, Sheldrick GM, Stalke D (2015) J Appl Cryst 48:3–10
26. SHELXT: Sheldrick GM (2015a) Acta Cryst A71:3–8
27. SHELXL: Sheldrick GM (2015b) Acta Cryst C71:3–8
28. ShelXle: a Qt graphical user interface for SHELXL, Hübschle CB, Sheldrick GM, Bittrich B (2011) J Appl Cryst 44:1281–1284.
29. Felder JB, Yeon J, Smith MD, zur Loye HC (2016) Inorg Chem 55:7167–7175
30. Suzuki S, Teshima K, Wakabayashi T, Nishikiori H, Yubuta K, Shishido T, Oishi S (2011) Cryst Growth Des 11:4825–4830
31. Wang X, Liu L, Wang X, Bai L, Chen C (2015) Cryst Eng Comm 17:925–929
32. Morrison G, Latshaw AM, Spagnuolo NR, zur Loye HC (2017) J Am Chem Soc 139:14743–14748
33. Latshaw AM, Wilkins BO, Morrison G, Smith MD, zur Loye HC (2016) J Solid State Chem 239:200–203
34. Welsch M, Babel D (1991) Z Naturforsch B 46:161–164